Kinetics of Malachite Green Fading in Alcohol–Water Binary Mixtures

BABAK SAMIEY, ALI RAOOF TOOSI

Department of Chemistry, Faculty of Science, University of Lorestan, 68137-17133, Khoramabad, Islamic Republic of Iran

Received 6 May 2009; revised 9 August 2009, 9 December 2009, 9 February 2010; accepted 22 February 2010

DOI 10.1002/kin.20500
Published online in Wiley InterScience (www.interscience.wiley.com).

ABSTRACT: The rate constant of alkaline fading of malachite green (MG^+) was studied in alcohol–water binary mixtures. This reaction was studied under pseudo-first-order conditions at 283–303 K. It was observed that the reaction rate constants were increased in the presence of different weight percentages of methanol, ethanol, 1-propanol, 2-propanol, ethylene glycol, 1,2-propanediol, and glycerol (up to 19.3%). In aqueous glycerol solutions higher than 19.3%, the rate constant of reaction slightly decreases, which is due to high viscosity values of solvent mixtures. The fundamental rate constants of MG^+ fading in these solutions were obtained by using the SESMORTAC model. Owing to the charged character of activated complex, with an increase in the weight percentage of the used cosolvents or temperature, k_2 values change according to the trend of hydroxide ion nucleophilic parameter values. Also, using MG^+ solvatochromism, a simple test, called MAGUS, is introduced for measuring the glycerol concentration in its aqueous solutions. © 2010 Wiley Periodicals, Inc. Int J Chem Kinet 42: 508–518, 2010

INTRODUCTION

Solvent effects on reactivity may be very large. Alcohols, as cosolvents, can change the rate of organic, inorganic, and enzymatic reactions [1–9]. Malachite green (MG^+) is a triphenylmethane dye. These dyes represent a class of dyes of commercial and analytical importance [10,11]. Malachite green is used to dye materials such as silk, leather, cotton, and paper and can be used as a saturable absorber in dye lasers, as a pH indicator or as a bacteriological stain [12]. It is also used as a topical antiseptic or to treat parasites and bacterial infections in fish and fish eggs [13]. In this work, we have studied the MG^+ alkaline fading in binary mixtures of water with different weight percentages of methanol, ethanol, 1-propanol, 2-propanol, ethylene glycol, 1,2-propanediol, and glycerol at 283–303 K. The MG^+ fading is a one-step reaction [14,15], and as reported kinetics of these kinds of reactions in binary mixtures can be studied using the SESMORTAC model [16].

EXPERIMENTAL

Materials

Malachite green oxalate, methanol (>99.5%), ethanol (≥99.9%), 1-propanol (≥99%), 2-propanol (≥99.5%), ethylene glycol (≥99%), 1,2-propanediol (≥99.5%), glycerol (≥99.5%), and NaOH were all purchased from Merck.

Correspondence to: B. Samiey; e-mail: babsamiey@yahoo.com.
Figures S1 and S2 and Tables S1–S3 are available as Supporting Information in the online issue at www.interscience.wiley.com.

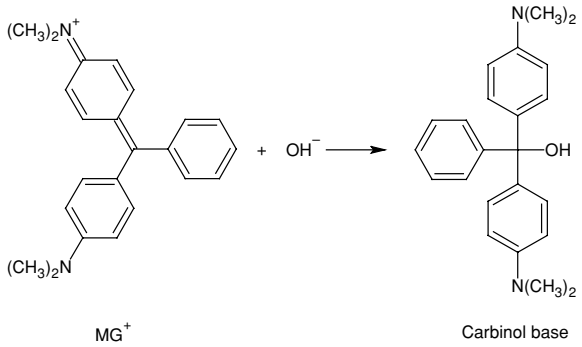

Scheme 1

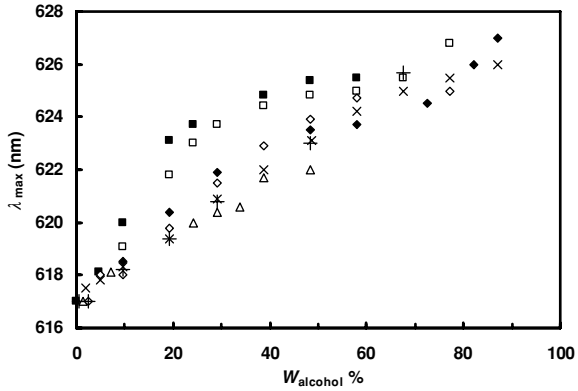

Figure 1 λ_{max} values of MG^+ vs. weight percentages of Δ, methanol; ♦, ethanol; ■, 1-propanol; □, 2-propanol; ×, ethylene glycol; ◇, 1,2-propanediol; and +, glycerol in water under alkaline conditions at room temperature.

Kinetic Procedure

The fading of MG^+ was followed at its maximum wavelength (λ_{max}) values in a thermostated cell compartment of a Shimadzu UV-1650PC spectrophotometer. The experiments were conducted at 283, 293, and 303 K within ±0.1 K in a stoppered cell. All the kinetic runs were carried out at least in triplicate. To perform each kinetic run, a 100-μL aliquot of 1.38×10^{-4} M MG^+ solution was added by a microsyringe into 2.9 mL of a solution containing 5.44×10^{-4} M sodium hydroxide and a certain concentration of alcohol. The reaction between MG^+ and hydroxide ion has been found to be bimolecular, first order with respect to each reactant, but pseudo-first-order conditions (excess alkali) were used in all cases (Scheme 1).

RESULTS AND DISCUSSION

The reaction of MG^+ with hydroxide ion brings about fading the color of MG^+ and results in the formation of colorless carbinol base (Scheme 1). In this work, we studied the influence of various concentrations of a series of mono- and polyhydroxylic alcohols on the kinetics of MG^+ fading. These hydroxylic cosolvents were chosen to compare the effect of number of OH groups and chain length on the reaction rate. As seen in Fig. 1, with an increase in weight percentage of the cosolvents, the λ_{max} value of MG^+ shifts to red. The redshift has been previously reported for other compounds upon going from polar to apolar solvents, as a result of hydrophobic interaction [17]. A reaction of MG^+ fading is an electrophile–nucleophile combination reaction. The rate constants for these reactions are correlated by using the Ritchie equation [18,19]

$$\log k = \log k_0 + N_+ \qquad (1)$$

where k is the rate constant for the reaction of a given cation with a given nucleophilic system (i.e., given nucleophile in a given solvent). k_0 is the rate constant for the same cation with water in water, and N_+ is a parameter that is characteristic of the nucleophilic system and is independent of cation. This equation is applied to the reactions between nucleophiles and certain large and relatively stable organic cations in various solvents. k_0 values for MG^+ are 1.46×10^{-8} and 9.93×10^{-8} M^{-1} min^{-1} at 283 and 303 K, respectively [15]. N_+ values obtained for hydroxide ion in the MG^+ fading reaction increase with an increase in the alcohol weight percentage (except for zone 3 of glycerol–water mixtures) and decrease with an increase in the temperature, as shown in footnotes of Tables I–VII. As shown in Tables I–VII, with an increase in the content of cosolvents the rate constant of reaction increases. Alcohols have a lower dielectric constant than water and according to Hughes–Ingold rules for solvent effects in nucleophilic substitution reactions [20–22], formation of the neutral carbinol base from two oppositely charged reactants is more favorable in higher weight percentages of alcohols. Confirming this result, it has been found the rate constant of crystal violet (CV^+) fading decreases in urea–water mixtures where the dielectric constant increases [23] and increases in the presence of cosolvents such as ethylene glycol, 1,2-propanediol, ethanol [5], 2-methoxy ethanol [24], and tetrahydrofuran [25]. On the other hand, the reaction rate of bromophenol blue ($BPB^=$) fading, which forms charged product, decreases with an increase in the weight percentage of alcohol in a series of alcohol–water mixtures [16,26]. Thus, it seems that in this work, the formation of neutral product from charged reactants has a central role in increasing the reaction rate of MG^+ fading with an increase in the concentration of alcohols.

As seen in Tables I–VII and Fig. S1 in the Supporting Information, at the same molar ratios of alcohols

Table I k_{obs} and E_a Values of MG^+ Fading in Ethanol–Water Solutions at 283–303 K

			k_{obs} (M^{-1} min^{-1})			
W_{EtOH}%	[EtOH] (M)	[H_2O] (M)	283 K	293 K	303 K	E_a (kJ mol^{-1})
0.0	0.000	55.556	18.89 ± 1.03	46.98 ± 2.10	118.60 ± 4.97	65.5 ± 2.0
9.7	2.050	48.609	31.80 ± 5.70	73.40 ± 15.53	169.70 ± 8.07	59.7 ± 1.7
12.1	2.540	46.919	38.98 ± 2.60	86.97 ± 2.54	190.46 ± 3.74	56.5 ± 1.1
14.5	3.053	45.470	51.89 ± 6.80	105.19 ± 2.22	222.48 ± 4.77	51.9 ± 2.1
19.3	3.989	43.037	59.01 ± 3.54	128.02 ± 4.00	269.31 ± 5.80	54.1 ± 1.2
29.0	6.097	37.673	74.18 ± 3.3	170.81 ± 6.23	342.86 ± 13.38	54.6 ± 2.0
38.7	7.598	31.835	128.01 ± 2.80	269.22 ± 8.71	598.34 ± 8.85	54.9 ± 2.5
48.3	9.295	26.448	198.62 ± 38.54	533.47 ± 8.78	1055.69 ± 97.23	59.6 ± 5.2
58.0	10.884	21.131	399.16 ± 14.91	846.72 ± 6.20	1879.90 ± 140.05	55.2 ± 2.3
67.7	12.388	16.605	716.60 ± 48.53	1554.94 ± 182.64	2730.45 ± 617.14	47.8 ± 3.5

k_{mc} values are given in the box.
Zones 1 and 2 are in the range of 0–14.5% and 14.5–67.7%, respectively.
N_+ values are in the range of 9.11–11.09 and 9.08–10.44 at 283 and 303 K, respectively.

Table II k_{obs} and E_a Values of MG^+ Fading in 1-Propanol–Water Solutions at 283–303 K

			k_{obs} (M^{-1} min^{-1})			
W_{1-PrOH}%	[1-PrOH] (M)	[H_2O] (M)	283 K	293 K	303 K	E_a (kJ mol^{-1})
0.0	0.000	55.556	18.89 ± 1.03	46.98 ± 2.10	118.60 ± 4.97	65.5 ± 2.0
4.8	0.794	51.700	25.09 ± 1.70	55.97 ± 3.08	138.00 ± 3.31	60.7 ± 3.5
9.7	1.581	48.724	35.08 ± 2.69	80.89 ± 1.90	170.47 ± 7.02	56.4 ± 1.5
19.3	3.066	42.781	49.60 ± 1.80	93.15 ± 2.52	196.85 ± 2.00	49.1 ± 3.5
24.2	3.786	39.598	68.29 ± 1.82	124.95 ± 2.04	209.31 ± 4.00	39.9 ± 1.3
29.0	4.493	37.042	101.81 ± 1.97	198.14 ± 2.28	382.18 ± 13.60	47.1 ± 1.1
38.7	5.857	31.353	172.07 ± 2.47	320.28 ± 1.47	654.69 ± 11.85	47.6 ± 3.0
48.3	7.157	25.803	365.05 ± 5.78	710.60 ± 4.43	1389.66 ± 34.15	47.6 ± 1.4
58.0	8.398	20.440	539.46 ± 53.16	1058.04 ± 27.93	1705.83 ± 335.12	41.1 ± 3.3

k_{mc} values are given in the box.
Zones 1 and 2 are in the range of 0–19.3% and 19.3–58.0%, respectively.
N_+ values are in the range of 9.11–10.57 and 9.08–10.23 at 283 and 303 K, respectively.

Table III k_{obs} and E_a values of MG^+ fading in 2-propanol–water solutions at 283–303 K

			k_{obs} (M^{-1} min^{-1})			
$W_{2\text{-}PrOH}$%	[2-PrOH] (M)	[H_2O] (M)	283 K	293 K	303 K	E_a (kJ mol^{-1})
0.0	0.000	55.556	18.89 ± 1.03	46.98 ± 2.10	118.60 ± 4.97	65.5 ± 2.0
9.7	1.518	48.437	24.16 ± 1.01	54.30 ± 1.30	131.50 ± 7.50	60.3 ± 2.8
19.3	2.951	43.013	24.00 ± 9.06	54.00 ± 1.08	145.00 ± 4.19	64.0 ± 5.1
24.2	3.638	39.831	25.97 ± 1.16	64.05 ± 1.10	154.46 ± 7.72	63.5 ± 1.5
29.0	4.308	37.078	50.00 ± 3.08	96.60 ± 3.28	207.70 ± 8.72	50.7 ± 3.3
38.7	5.599	31.438	56.85 ± 5.65	117.58 ± 8.79	275.48 ± 10.56	56.2 ± 3.8
48.3	6.862	25.893	69.67 ± 11.31	166.93 ± 14.40	400.86 ± 27.70	62.4 ± 1.7
53.2	7.418	23.462	114.61 ± 2.15	257.94 ± 7.25	600.63 ± 61.14	59.0 ± 2.2
58.0	8.035	20.451	266.45 ± 31.02	580.99 ± 63.45	1221.66 ± 56.59	54.3 ± 1.1
67.7	9.106	15.804	658.32 ± 69.83	1106.17 ± 149.34	1893.18 ± 452.12	37.6 ± 1.3

k_{mc} values are given in the box.
Zones 1 and 2 are in the range of 0–24.2% and 24.2–67.7%, respectively.
N_+ values are in the range of 9.11–10.66 and 9.08–10.28 at 283 and 303 K, respectively.

Table IV k_{obs} and E_a Values of MG^+ Fading in Methanol–Water Solutions at 283–303 K

			k_{obs} (M^{-1} min^{-1})			
W_{MeOH}%	[MeOH] (M)	[H_2O] (M)	283 K	293 K	303 K	E_a (kJ mol^{-1})
0.0	0.000	55.556	18.89 ± 1.03	46.98 ± 2.10	118.60 ± 4.97	65.5 ± 2.0
1.0	0.309	54.153	44.28 ± 2.36	89.12 ± 7.63	179.44 ± 17.47	49.9 ± 1.4
1.5	0.454	53.946	65.56 ± 4.03	122.10 ± 1.75	242.50 ± 9.74	46.6 ± 2.4
2.4	0.758	53.857	117.46 ± 7.63	210.65 ± 6.18	367.47 ± 16.70	40.7 ± 0.8
4.8	1.503	52.196	122.14 ± 1.72	229.66 ± 4.80	420.22 ± 19.51	44.0 ± 0.9
9.7	2.943	48.385	289.88 ± 7.38	528.09 ± 6.33	968.03 ± 33.78	43.0 ± 1.3
14.5	4.365	45.795	526.92 ± 9.94	947.32 ± 17.86	1398.90 ± 46.65	34.9 ± 3.4
19.3	5.747	42.661	583.43 ± 50.25	1126.11 ± 63.65	2054.88 ± 14.77	44.9 ± 0.9
24.2	7.394	39.710	691.66 ± 22.40	1367.75 ± 18.41	2514.45 ± 40.15	46.0 ± 1.1
29.0	8.388	37.044	788.91 ± 8.18	1560.28 ± 27.67	2738.51 ± 144.54	44.4 ± 1.8
33.8	9.672	33.930	1022.64 ± 23.00	2015.58 ± 52.07	3536.95 ± 174.43	44.3 ± 1.8
38.7	10.914	31.541	1213.87 ± 21.62	2164.47 ± 473.48	4656.86 ± 204.45	47.8 ± 4.9
48.3	13.326	26.332	1419.35 ± 93.33	3104.81 ± 68.99	5654.61 ± 313.53	49.3 ± 3.0

k_{mc} values are given in the boxes.
Zones 1, 2, and 3 are in the range of 0–2.4%, 2.4–14.5%, and 14.5–48.3%, respectively.
N_+ values are in the range of 9.11–10.99 and 9.08–10.76 at 283 and 303 K, respectively.

Table V k_{obs} and E_a Values of MG^+ Fading in Ethylene Glycol–Water Solutions at 283–303 K

			k_{obs} (M^{-1} min^{-1})			
W_{eg}%	[eg] (M)	[H_2O] (M)	283 K	293 K	303 K	E_a (kJ mol^{-1})
0.0	0.000	55.556	18.89 ± 1.03	46.98 ± 2.10	118.60 ± 4.97	65.5 ± 2.0
1.0	0.179	55.255	33.47 ± 1.22	54.98 ± 3.37	144.47 ± 12.20	51.9 ± 10.7
1.9	0.292	54.062	39.47 ± 1.25	65.89 ± 2.98	156.37 ± 4.89	48.9 ± 8.1
2.4	0.395	53.407	56.98 ± 1.16	83.60 ± 3.19	180.26 ± 1.45	40.9 ± 8.8
4.8	0.788	52.445	82.53 ± 3.41	163.78 ± 6.72	279.00 ± 7.15	43.5 ± 2.4
9.7	1.577	50.139	108.04 ± 3.10	202.23 ± 11.73	369.89 ± 9.56	43.9 ± 1.0
14.5	2.372	47.742	123.35 ± 4.99	249.43 ± 1.08	400.00 ± 68.2	42.0 ± 4.0
19.3	3.181	45.027	134.45 ± 4.30	264.00 ± 13.10	419.11 ± 16.41	40.6 ± 3.7
29.0	4.817	40.230	139.59 ±1.33	286.72 ± 6.94	487.54 ± 7.38	44.6 ± 3.1
38.7	6.491	35.093	143.00 ± 5.74	302.17 ± 3.97	573.77 ± 18.39	49.5 ± 1.6
48.3	8.202	29.702	147.14 ± 5.5	312.56 ± 3.55	610.00 ± 20.31	50.7 ± 1.3
58.0	9.952	24.349	158.54 ± 2.41	347.70 ± 12.62	698.94 ± 11.17	52.9 ± 1.3
67.7	11.717	18.988	212.81 ± 11.09	425.05 ± 13.82	898.57 ± 13.31	51.3 ± 2.4
77.3	13.536	13.439	266.62 ± 6.57	544.95 ± 12.10	1110.25 ± 27.34	52.5 ± 1.4
87.0	15.392	7.844	374.25 ± 14.04	780.12 ± 8.83	1493.86 ± 56.52	49.4 ± 0.7

[eg] = Ethylene glycol.
k_{mc} values are given in the boxes.
Zones 1, 2, and 3 are in the range of 0–4.8%, 4.8–19.3%, and 19.3–87.0%, respectively.
N_+ values are in the range of 9.11–10.41 and 9.08–10.18 at 283 and 303 K, respectively.

and temperatures, the rate constants of the MG^+ fading reaction in the low mole ratios of alcohols change as follows:

$$k_w < k_{2-\mathrm{PrOH}} \approx k_{\mathrm{EtOH}} < k_{1-\mathrm{PrOH}} \approx k_{\mathrm{prd}} < k_{\mathrm{Gl}} < k_{\mathrm{eg}} \leq k_{\mathrm{MeOH}} \quad (2)$$

where $k_{\mathrm{MeOH}}, k_{\mathrm{eg}}, k_{\mathrm{Gl}}, k_{\mathrm{prd}}, k_{1-\mathrm{Pr\,OH}}, k_{\mathrm{EtOH}}, k_{2-\mathrm{PrOH}}$, and k_w are the rate constants of the MG^+ fading reaction in aqueous mixtures of methanol, ethylene glycol, glycerol, 1,2-propanediol, 1-propanol, ethanol, 2-propanol, and in water, respectively. In relation (2), it seems that affinity of hydroxide ions and thus, the rate constants of the MG^+ fading increase approximately according

Table VI k_{obs} and E_a Values of MG^+ Fading in 1,2-Propanediol–Water Solutions at 283–303 K

			k_{obs} (M^{-1} min^{-1})			
W_{prd}%	[prd] (M)	[H_2O] (M)	283 K	293 K	303 K	E_a (kJ mol^{-1})
0.0	0.000	55.556	18.89 ± 1.03	46.98 ± 2.10	118.60 ± 4.97	65.5 ± 2.0
0.3	0.048	54.516	28.00 ± 1.21	66.44 ± 2.95	148.45 ± 3.73	59.5 ± 1.2
1.0	0.155	54.342	29.99 ± 1.70	70.87 ± 2.20	158.99 ± 6.81	59.5 ± 1.2
2.4	0.396	53.569	35.09 ± 5.70	77.77 ± 4.22	177.13 ± 14.32	57.7 ± 2.0
7.3	1.170	51.065	37.43 ± 6.89	84.60 ± 4.46	192.49 ± 2.97	58.3 ± 1.7
9.7	1.556	49.683	40.64 ± 0.94	92.53 ± 2.12	196.69 ± 7.56	56.2 ± 1.2
19.3	3.135	44.546	60.89 ± 2.32	122.50 ± 1.97	239.28 ± 5.51	48.8 ± 1.1
29.0	4.715	39.593	64.73 ± 2.55	142.53 ± 3.24	287.10 ± 5.68	53.1 ± 1.3
38.7	6.306	34.431	73.42 ± 2.67	156.79 ± 9.59	312.10 ± 6.75	51.6 ± 1.2
48.3	7.902	29.125	87.70 ± 2.95	199.27 ± 5.01	422.58 ± 8.29	56.1 ± 1.2
58.0	9.514	23.844	111.48 ± 5.28	259.44 ± 3.43	555.14 ± 24.85	57.2 ± 1.3
67.7	11.131	18.332	175.37 ± 1.77	395.26 ± 8.17	798.20 ± 12.57	54.0 ± 1.6
77.3	12.759	12.699	296.78 ± 1.16	640.73 ± 7.93	1212.13 ± 18.03	50.2 ± 2.0

[prd] = 1,2-Propanediol.
k_{mc} values are given in the boxes.
Zones 1, 2, and 3 are in the range of 0–2.4%, 2.4–19.3%, and 19.3–77.3%, respectively.
N_+ values are in the range of 9.11–10.31 and 9.08–10.09 at 283 and 303 K, respectively.

Table VII k_{obs} and E_a Values of MG^+ Fading in Glycerol–Water Solutions at 283–303 K

			k_{obs} (M^{-1} min^{-1})			
W_{Gl}%	[Gl] (M)	[H_2O] (M)	283 K	293 K	303 K	E_a (kJ mol^{-1})
0.0	0.000	55.556	18.89 ± 1.03	46.98 ± 2.10	118.60 ± 4.97	65.5 ± 2.0
0.7	0.142	54.433	33.67 ± 1.56	68.00 ± 6.27	149.67 ± 9.86	53.1 ± 3.0
1.3	0.279	54.342	38.83 ± 2.66	73.11 ± 2.73	167.46 ± 1.75	52.0 ± 5.2
2.4	0.529	53.858	47.67 ± 4.23	99.67 ± 8.03	206.67 ± 10.07	52.3 ± 1.3
4.8	1.059	51.237	61.10 ± 1.35	125.37 ± 1.76	222.38 ± 7.80	46.1 ± 2.3
9.7	2.141	50.757	65.40 ± 3.48	131.35 ± 2.77	236.88 ± 11.46	45.9 ± 1.6
14.5	3.253	48.576	70.07 ± 4.09	141.73 ± 2.42	252.70 ± 5.90	45.8 ± 1.9
19.3	4.379	46.267	74.16 ± 4.56	159.69 ± 6.76	308.84 ± 8.02	50.9 ± 1.6
29.0	6.771	41.398	71.08 ± 1.67	150.58 ± 5.16	291.90 ± 1.90	50.4 ± 1.3
48.3	11.704	31.701	62.79 ± 1.49	135.17 ± 5.60	280.60 ± 1.20	53.4 ± 1.1
67.7	17.200	20.298	60.12 ± 2.26	130.97 ± 1.35	264.33 ± 3.10	52.8 ± 1.2

[GI] = Glycerol.
k_{mc1} and k_{mc3} values are given in the boxes.
Zones 1, 2, and 3 are in the range of 0–4.8%, 4.8–19.3%, and 19.3–67.7%, respectively.
N_+ values are in the range of 9.11–9.62 and 9.08–9.43 at 283 and 303 K, respectively.

to a decrease in hydrophobicity of the used alcohols [27–29].

In high mole ratios of alcohols, reaction rates change as follows:

$$k_w < k_{Gl} < k_{prd} \leq k_{eg} < k_{2-PrOH} \leq k_{EtOH} < k_{1-PrOH} \ll k_{MeOH} \quad (3)$$

To interpret these facts, it can be said MG^+ is a triphenyl methyl dye with two $(CH_3)_2N$-substituted phenyl groups attached to the positively charged *tert*-carbon atom at the center and has quinoid resonating forms and its solvation in aqueous mixtures of different cosolvents is likely to be an involved process. Because of the large size of MG^+ and the low surface charge density around this large-sized ion, electrostatic interactions seem negligibly small and dispersion interaction is likely most effective factor in MG^+ solvation. However, the extent of hydrogen-bonding interactions in aquo-organic mixtures is likely to determine the accessibility of the hydrophobic portion

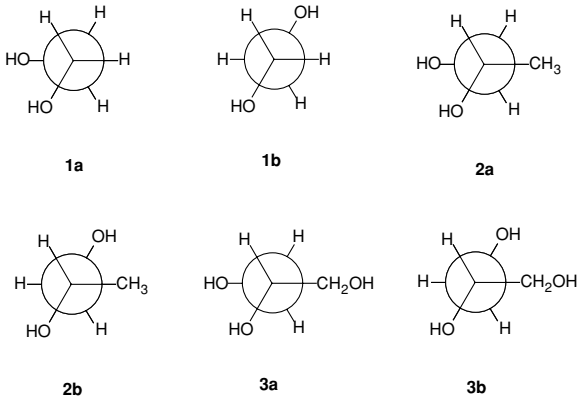

Scheme 2

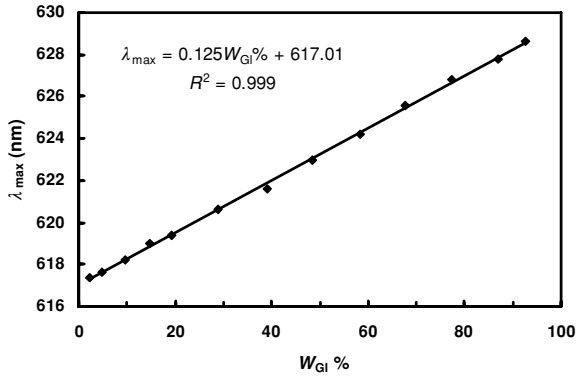

Figure 2 λ_{max} values of MG^+ vs. weight percentages of glycerol in water under neutral conditions at room temperature.

of the organic cosolvent molecule for dispersion interaction. Thus, the presence of the increased number of hydrogen-bonding centers is likely to decrease the hydrophobicity of an organic cosolvent molecule in aqueous mixtures and thus reduce the magnitude of dispersion interaction with an organic solute. It seems that the approach of the large MG^+ molecule toward the hydrophobic methylene chain of polyhydroxylic alcohols is sterically hindered owing to OH groups of alcohol molecules, as it is expected from conformational structures of ethylene glycol (**1a**) and (**1b**), 1,2-propanediol (**2a**) and (**2b**), and glycerol (**3a**) and (**3b**), as shown in Scheme 2. Steric hindrance due to the position of the OH group reduces the hydrophobic interaction between MG^+ and a methylene chain of 2-propanol compared to that of 1-propanol and results in a decrease in the rate constant of the fading reaction compared to 1-propanol.

On the other hand, in relation (3), the rate constants of MG^+ fading decrease approximately according to the increase in viscosity of the alcohols used [30]. It seems that with an increase in viscosity of solvents, mobility of reactants decreases and as observed in relation (3), the rate constants of MG^+ fading in polyhydroxylic alcohols (with high viscosity values) are less than those of monohydroxylic alcohols.

As shown in Table VII, the rate constants of the MG^+ fading reaction in aqueous glycerol mixtures up to 19.3% increase and then slightly decrease. Similar situation has been found for crystal violet fading in glycerol–water mixtures [19,31]. As reported, reaction rates decrease with an increase in viscosity of solvent [32,33]. Thus, it seems that an increase in the glycerol concentration results in a decrease in dielectric constant of a mixed solvent and a dramatic increase in the solvent viscosity, which in the former case increases the reaction rate and the latter decreases it. Competition between these two effects finally results in the observed decrease in the reaction rate in glycerol weight percentages above 19.3%. As shown in Fig. 1, over a wide concentration range of ethylene glycol, 1,2-propandiol, and glycerol, which have high viscosity values, there is a linear relation between the redshift of λ_{max} values of MG^+ and their concentrations in their aqueous solutions. On the other hand, it was observed that in the absence of NaOH, this relation holds over most of the concentration range of glycerol (Fig. 2). This test shows that in spite of hydrophobic interactions that occurred between MG^+ and glycerol molecules, the reaction rate decreases, which is due to high viscosity values of glycerol solutions. This test, called MAGUS, is explained in the Appendix and can be used for measuring the glycerol concentration in its aqueous solutions.

Proposed Reaction Mechanism

Data of Tables I–VII were analyzed by using the SESMORTAC model. In the SESMORTAC model [16], a range of solvent composition in which the equation of logarithm of reaction rate constant, $\log k$, versus reciprocal of the dielectric constant of the solution, D^{-1}, is linear [34–41], is called a "zone" and a solvent composition in which a zone finishes and another zone starts, which is called "*m*echanism *c*hange point" (abbreviated as *mc* point). Consideration of a mechanism on the basis of point charge on a dielectric continuum suggests that the plots of $\log k$ against D^{-1} should be linear. The failure of the simple electrostatic interpretation shows the importance of hydrogen bonding and other nonelectrostatic medium effects in controlling the reactivity of the substrates [40,42]. In such cases, the differential solvation of the initial and transition states is the controlling factor for changes in the rate constant with the solvent composition. In the SESMORTAC model,

variation in mechanism is followed through the study of changes in microenvironment (or solvent cage) of the activated complex. Dielectric constants of the used alcohol–water solutions are obtained from the works of Verbeek et al. [43] and Åkerlof [44].

It is found that in the used concentration range of alcohols, mixtures of water with ethanol, 1-propanol, and 2-propanol were two-zone and aqueous mixtures of methanol, 1,2-propanediol, ethylene glycol, and glycerol were three-zone. As seen from Tables I–VII, E_{act} values decrease sharply at the boundary of zones. On the other hand, difference between activation free energies of the reaction in solvent systems and water, $\Delta G_t^{\neq}$, can be obtained by applying the Eyring equation as follows:

$$\Delta G_t^{\neq} = \Delta G_S^{\neq} - \Delta G_W^{\neq} = RT \ln(k_w/k_s) \qquad (4)$$

where $\Delta G_S^{\neq}$ and $\Delta G_W^{\neq}$ are the free energies of activation in solvent systems and water, respectively. k_w and k_s are the reaction rate constants in water and solvent systems, respectively. As seen in Fig. 3, in all cases $\Delta G_t^{\neq}$ values of the MG^+ fading reaction are negative and change sharply about boundary of zones. It suggests that the system is more stabilized when water is replaced by the alcohol–water mixture.

As shown in Tables S1 and S2 in the Supporting Information, $\Delta S^{\neq}$ (except for the zone 3 of glycerol–water mixtures) and $\Delta H^{\neq}$ values reach their minimum values about the boundaries of zones. These may be due to the dissolution of alcohol molecules in the solvent cage [45–50] and nonelectrostatic, especially hydrophobic interactions [51], between MG^+ and alcohol molecules when ACSM forms. ACSM is an abbreviation for "*a*ctivated *c*omplex formed in the *s*econd *m*echanism" and will be explained later. It is seen that in each region of alcohol–water systems, there is a linear relation between $\Delta S^{\neq}$ and $\Delta H^{\neq}$ values of the fading reaction (Figs. S2(a)–(g) and Table S3 in the Supporting Information) and therefore a compensation effect between them that results in the weak dependence of $\Delta G^{\neq}$ upon composition of the used alcohols. As seen in Table S2 in the Supporting Information, $\Delta S^{\neq}$ value of the fading reaction in water is positive. As found in [34], for reactions between oppositely charged ions, there is an increase in the $\Delta S^{\neq}$ value going from reactants to activated complex. Thus, the activated complex has less charge than the reactants and will be partially desolvated [34]. It seems that negative $\Delta S^{\neq}$ values in alcohol–water binary mixtures (Table S2 in the Supporting Information) are due to solvation of activated complex by alcohol molecules added to ACSM in each zone, which support the formation of more ordered transition states compared to it in water.

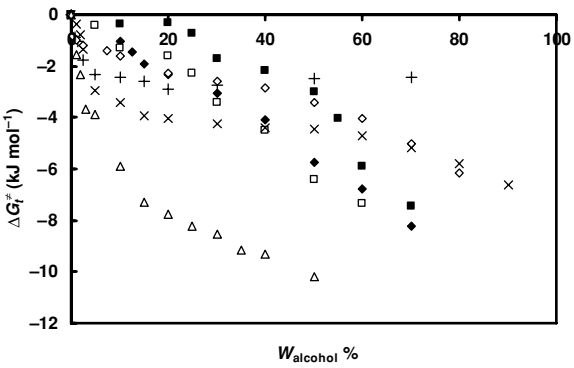

Figure 3 $\Delta G_t^{\neq}$ values of MG^+ fading reaction vs. weight percentages of Δ, methanol; ♦, ethanol; □, 1-propanol; ■, 2-propanol; ×, ethylene glycol; ◇, 1,2-propanediol; and +, glycerol in water under alkaline conditions at 293 K.

A large body of experimental data and theoretical calculations (e.g., of the Kirkwood–Buff integral functions) has shown that many aqueous binary mixtures are microheterogeneous, there exist microdomains composed of organic solvent surrounded by water, and of water solvated by organic solvent. The onset and composition of these microdomains depend on the pair of solvents. There exist the possibilities of solvation of the solute by one of the two solvent microdomains [52–56]. Thus, the composition of the solvation shell differs from that of bulk mixture [57], and there is a solvent exchange equilibrium between molecules of binary mixture components in the solvation shell of solute [58,59].

In aqueous organic mixtures, formation of 1:1 hydrogen-bonded species between organic and water molecules leads to the solvent exchange equilibria, which results in the preferential solvation of solute molecules [60]. The number of solvent molecules whose exchange in the solvatochromic indicator (or probe) solvation shell affects its solvent polarity scale is usually ≤ 2, and concentration of the solvent species are effective [60].

The solvent cage is the microenvironment of the $MG^{\delta+}$–$OH^{\delta-}$ contact pair and, in spite of the first solvation shell, includes many water and alcohol molecules, and its dielectric constant value is an intensive property. Thus, in each region, n molecules of water can be replaced by n molecules of alcohol. Here, two processes occur simultaneously, a chemical reaction between MG^+ and OH^- (first order in contact ion) and replacement of n water molecules of the ACSM microenvironment by n alcohol molecules of its surrounding (n order in solvent molecules); the progress of the first process is the driving force of the second one.

Table VIII n, k_1, k_{-1}, k_2, and $E_a(k_1)$ Values of Different Zones for the MG^+ Fading Reaction in Various Alcohol–Water Binary Mixtures Obtained from the SESMORTAC Model at Different Temperatures

	n			k_1 ($M^{-(n+1)}$ min^{-1})			k_{-1} (M^{-n} min^{-1})			k_2(min^{-1})			$E_a(k_1)$ (kJ mol^{-1})		
T (K)	1st	2nd	3rd	1st	2nd	3rd	1st	2nd	3rd	1st	2nd	3rd	1st	2nd	3rd
							Ethanol + water								
283	2.45	3.56	–	2.12	0.23	–	4.90E–5	3.28E–8	–	9.37E5	1.81E6	–			
293	2.00	3.22	–	6.26	1.07	–	2.63E–5	1.17E–7	–	6.43E5	1.10E6	–	65.9	99.8	–
303	1.83	3.01	–	13.42	3.77	–	1.24E–4	7.33	–	4.88E5	7.58E5	–			
							1-Propanol + water								
283	1.75	2.13	–	11.05	15.58	–	9781.57	1.50E–5	–	9781.57	4.64E5	–			
293	3.90	2.22	–	33.85	26.65	–	1769.44	1.11E–5	–	1769.44	3.81E5	–	53.3	41.5	–
303	2.36	2.24	–	48.89	50.01	–	5647.15	5.01E–6	–	5647.15	2.98E5	–			
							2-Propanol + water								
283	RC	7.74	–	–	0.011	–	RC	5.01E–3	–	–	3.91E7	–			
293	RC	7.31	–	–	0.053	–	RC	3.31E–2	–	–	4.24E7	–	–	96.0	–
303	1.20	7.19	–	7.49	0.162	–	1.50E–4	0.101	–	6.07E5	5.42E7	–			
							Methanol + water								
283	1.49	4.19	2.97	147.98	16.26	6.39	4.82E–4	1.34E3	797.41	2.71E5	1.11E6	1.42E6	33.1	90.2	134.9
293	1.53	3.17	1.50	264.59	49.29	79.97	5.01E3	1.61E3	1.38E–5	1.92E5	4.14E5	2.53E5			
303	1.47	3.93	1.26	375.69	205.34	277.32	8.26E–4	2437.75	84.58	1.58E5	2.99E5	1.57E5			
							Ethylene glycol + water								
283	0.97	0.84	3.41	81.29	36.43	0.05	1.85E–3	2.85E4	6.59E–9	3.96E5	3.35E5	3.53E6	36.0	46.8	168.8
293	1.77	2.17	3.16	184.33	89.41	0.13	1.03E3	1.39E4	1.37E–7	2.39E5	2.18E5	1.77E6			
303	1.37	0.56	2.07	221.84	134.71	5.90	5.35E–4	3.62E4	4.27E–6	2.01E5	1.96E5	6.46E5			
							1,2-Propanediol + water								
283	0.29	2.28	3.63	20.73	4.35	0.06	7.40E–3	4.47E3	5.70E–8	4.73E5	9.95E5	3.10E6			
293	0.22	2.30	3.10	37.42	13.67	0.46	0.004	8.09E3	1.33E–7	4.45E5	6.06E5	8.18E5	47.4	50.9	135.0
303	0.33	1.23	2.60	78.63	17.97	2.64	2.42E–3	6.42E–4	5.61E–7	3.00E5	4.89E5	7.84E5			
							Glycerol + water								
283	0.54	1.18	3.47	40.78	3.98	6.60E–4	1.64E–4	2.98E4	2.50E3	3.53E5	7.62E5	6.24E6			
293	0.82	1.68	3.03	86.79	4.55	2.81E–3	0.005	1.68E–4	4.79E2	3.19E5	7.27E5	1.22E6	46.2	17.0	235.4
303	0.84	2.19	1.36	148.81	6.43	0.51	1.16E–3	2.52E–4	1.55E–4	2.36E5	6.52E5	1.67E5			

RC, Rate constant is approximately constant.
E_a (k_1) values are activation energy of k_1 values.

As described in the theory of the SESMORTAC model (and as seen in Table VIII), the values of n are different from one region to the next one and this causes a break in the plot of log k vs. D^{-1} at each *mc* point. In computational chemistry, a computed continuum solvent may be considered between each two successive *mc* points and *mc* points may be assumed as nodal points.

In this reaction, the solvent is not a reactant. Thus, because of the SESMORTAC model, this reaction is of type I. In the MG^+ fading reaction, in the presence of the used alcohols (except for the zone 3 of glycerol–water mixtures) the reaction rate increases and the proposed mechanism for the MG^+ fading reaction in these solutions involves two kinds of mechanisms.

The first mechanism occurs in pure solvent. Starting in the first zone, this mechanism can be written as follows:

$$[(MG^+ + OH^-)]_{cage} \underset{k'_{-1}}{\overset{k'_1}{\rightleftarrows}} \left[\left(MG^{\delta+}_{AC} - OH^{\delta-}\right)\right]^{\neq}_{cage} \xrightarrow{k'_2} \text{Product} \quad (5)$$

where AC is activated complex; k'_1, k'_{-1}, and k'_2 are the fundamental rate constants of the MG^+ fading reaction, and we cannot determine them. The related rate equation, v_1, is written as follows:

$$v_1 = k[MG^+][OH^-] \quad (6)$$

where k is the observed rate constant in water.

Adding alcohol to a reaction medium results in formation of ACSM and increases the reaction rate. The second mechanism is written as follows:

$$[MG^+ + OH^-)\cdot nH_2O]_{cage} + nS \underset{k_{-1}}{\overset{k_1}{\rightleftarrows}} \left[\left(MG^{\delta}_{ACSM} - OH^{\delta-}\right)\cdot nS\right]^{\neq}_{cage} + nH_2O \xrightarrow{k_2} \text{Product} \quad (7)$$

where alcohol molecules are shown by S and k_1, k_{-1}, and k_2 are the fundamental rate constants of the MG^+ fading reaction in alcohol–water binary mixtures. In each binary mixture, structure of ACSM depends on the structure of solvent cage. Dielectric constant values of alcohols are less than that of water and when ACSM forms in each zone, n molecules of water existing in the solvent cage are replaced by n molecules of alcohol from its surrounding. This decreases the dielectric constant value of the microenvironment of $(MG^{\delta+} - OH^{\delta-})$ in ACSM, and formation of neutral product, MGOH, is more favorable. This results in an increase in the rate of the fading reaction. In the first zone, assuming that a steady-state concentration of ACSM is reached in the used binary mixtures, we have

$$[ACSM] = \frac{k_1^1[MG^+][OH^-][S]^n}{k_{-1}^1[H_2O]^n + k_2^1} \quad (8)$$

The effect of alcohol molecules to the reaction rate equation in the first zone, v_2, is as follows:

$$v_2 = k_2^1[ACSM] = \frac{k_1^1k_2^1[MG^+][OH^-][S]^n}{k_{-1}^1[H_2O]^n + k_2^1} \quad (9)$$

and the equation of reaction rate in binary mixtures, v, is

$$v = v_1 + v_2 = k_{obs}[MG^+][OH^-] = \left(k + \frac{k_1^1k_2^1[S]^n}{k_{-1}^1[H_2O]^n + k_2^1}\right)[MG^+][OH^-] \quad (10)$$

where

$$k_{obs} = k + \frac{k_1^1k_2^1[S]^n}{k_{-1}^1[H_2O]^n + k_2^1} \quad (11)$$

k_{obs} and k are the second-order rate constant in a binary mixture and water, respectively, and k_1^1, k_{-1}^1, and k_2^1 are the fundamental rate constants of the MG^+ fading reaction in the first zone. In the second zone, Eq. (11) is replaced by

$$k_{obs} = k_{mc_1} + \frac{k_1^2k_2^2\left([S] - [S]_{mc_1}\right)^n}{k_{-1}^2\left([H_2O]_{mc_1} - [H_2O]\right)^n + k_2^2} \quad (12)$$

where

$$k_{mc_1} = k + \frac{k_1^1k_2^1[S]^n_{mc_1}}{k_{-1}^1[H_2O]^n_{mc_1} + k_2^1} \quad (13)$$

$[S]_{mc_1}$ and $[H_2O]_{mc_1}$ are the concentrations of alcohol and water in mc_1 point, respectively, and k_1^2, k_{-1}^2, and k_2^2 are the fundamental rate constants of the MG^+ fading reaction in the second zone. The second term in Eq. (12) shows the effect of alcohol molecules on the rate equation in the second zone. k_{obs} values of the third zones of methanol, ethylene glycol, and 1,2-propanediol aqueous mixtures are obtained as follows:

$$k_{obs} = k_{mc_2} + \frac{k_1^3k_2^3\left([S] - [S]_{mc_2}\right)^n}{k_{-1}^3\left([H_2O]_{mc_2} - [H_2O]\right)^n + k_2^3} \quad (14)$$

where

$$k_{mc_2} = k + \frac{k_1^1k_2^1[S]^n_{mc_1}}{k_{-1}^1[H_2O]^n_{mc_1} + k_2^1} + \frac{k_1^2k_2^2\left([S]_{mc_2} - [S]_{mc_1}\right)^n}{k_{-1}^2\left([H_2O]_{mc_1} - [H_2O]_{mc_2}\right)^n + k_2^2} \quad (15)$$

$[S]_{mc_2}$ and $[H_2O]_{mc_2}$ are the concentrations of alcohol and water in mc_2 point, respectively, and k_1^3, k_{-1}^3, and k_2^3 are the fundamental rate constants of the MG^+ fading reaction in the third zone. The second term in Eq. (14) shows the effect of alcohol molecules on the rate equation in the third zone.

In zone 3 of the glycerol–water solvent system, the reaction rate decreases with an increase in the glycerol concentration and k_{mc_3} is the lowest observed rate constant in the third zone. In this zone, it is assumed that n molecules of glycerol existing in the solvent cage are replaced by n molecules of water from its surrounding and the following equation is used for the second mechanism:

$$k_{obs} = k_{mc3} + \frac{k_1^3k_2^3\left([H_2O] - [H_2O]_{mc3}\right)^n}{k_{-1}^3\left([S]_{mc3} - [S]\right)^n + k_2^3} \quad (16)$$

where the second term in Eq. (16) shows the contribution of water molecules on the reaction rate in this zone. Also, it has been shown that k_1 values in each zone obey the Arrhenius equation [16] and the related activation energy, $E_a(k_1)$, values are given in Table VIII. Data

of the first zone fitted properly in Eq. (11), those of the second and third zones fitted suitably in Eqs. (12), (14), and (16), and the results are given in Table VIII. As seen in Table VIII, at each certain temperature, k_1 values decrease with an increase in the alcohol concentration from zone 1 to higher zones. To interpret this fact, we may say an increase in alcohol concentration decreases both dissociation of reactants into their constituent ions and mobility of ions which in most cases results in an increase in $E_a(k_1)$ values from zone 1 to higher zones (Table VIII). It is found that k_2 values increase with an increase in the alcohol concentration from zone 1 to higher zones because the formation of neutral carbinol base from partially charged activated complex [61] is more favorable with an increase in the alcohol concentration. Also, k_2 values decrease with an increase in the temperature in each certain zone. As seen in Tables I–VIII, with an increase in the weight percentage of the used cosolvents or temperature, k_2 values change according to the trend of hydroxide ion nucleophilic parameter, N_+, values.

CONCLUSIONS

The rate constant of the MG^+ fading reaction increases in the presence of methanol, ethanol, 1-propanol, 2-propanol, ethylene glycol, 1,2-propanediol, and glycerol (up to 19.3%). But it is found that in aqueous glycerol solutions higher than 19.3%, the rate constant of reaction slightly decreases, which is due to their high viscosity values. The fundamental rate constants of the MG^+ fading reaction in the used solvent systems are obtained by the SESMORTAC model. It is observed that k_2 values change according to the trend of hydroxide ion nucleophilic parameter values and at each certain temperature, k_1 values decrease from zone 1 to higher zones. On the other hand, using MG^+ solvatochromism, a simple test, called MAGUS, was introduced for measuring the glycerol concentration in its aqueous solutions.

APPENDIX

Measuring Aqueous Glycerol Concentration Using Dye Solvatochromism (MAGUS) Test

As seen in Figs. 1 and 2, there is a linear relation between λ_{max} values of MG^+ and weight percentages of glycerol (abbreviated as $\lambda_{max} - W_{Gl}\%$ relation) in both alkaline and neutral aqueous glycerol solutions at room temperature, which can be used for measuring aqueous glycerol concentration. It is good to say that MAGUS is an ancient Persian word meaning wise man and holy man. Tests show that the $\lambda_{max} - W_{Gl}\%$ relation does not hold over the concentration range of 0–1%, where the λ_{max} value of MG^+ remains constant at 617 nm. To carry out the MAGUS test, a 100-μL aliquot of 1.38×10^{-4} M MG^+ solution is added by a microsyringe into 2.9 mL of an unknown concentration aqueous glycerol solution and the λ_{max} value of MG^+ is measured. Then, using the $\lambda_{max} - W_{Gl}\%$ relation and considering the dilution effect in measuring cell, the glycerol concentration is calculated. The concentration of glycerol in a series of samples was measured, and the results are presented in Table A1. The experimental and calculated data were compared by statistical paired t-test and regression line methods, and no significant difference was observed.

Table A.1 Measuring Glycerol Concentration in a Series of Samples by the MAGUS Test

$W_{Gl}\%$ in samples		
Prepared	Calculated	λ_{max} (nm)
1.1	1.5	617.2
2.5	3.1	617.4
7.7	8.1	618.0
17.1	16.4	619.0
23.6	23.0	619.8
44.8	44.5	622.4
64.9	64.4	624.8
84.9	85.9	627.4
95.0	94.2	628.4

SUPPORTING INFORMATION

The following data are presented as Supporting Information in the online issue at www.interscience.wiley.com:

- Figure S1 shows k_{obs} values of the MG^+ fading reaction in terms of different mole ratios of the used alcohols in water at 293 K. Figures S2a–S2g show the compensation plots of $\Delta S^{\neq}$ versus $\Delta H^{\neq}$ values of the MG^+ fading reaction in different weight percentages of the used alcohols in water.
- In Table S1, $\Delta H^{\neq}$ values, in Table S2 $\Delta S^{\neq}$ values, and in Table S3 equations of the compensation effect between $\Delta S^{\neq}$ and $\Delta H^{\neq}$ values of the MG^+ fading reaction in different weight percentages of the used alcohols in water are presented.

BIBLIOGRAPHY

1. Iwanaga, R. Bull Chem Soc Japan 1962, 35, 869.
2. Wada, G.; Kobayashi, Y. Bull Chem Soc Japan 1975, 48, 2451.
3. Raff, R. A.V.; Silverman, B. H. Can J Chem 1951, 29, 857.
4. Brinchi, L.; Di Profio, P.; Germani, R.; Salvelli, G.; Spreti, N. J Colloid Interface Sci 2002, 247, 429.
5. Yesin, T. R.; Sinem, G.; Melda, T. Colloids Surf A 2005, 270–271, 72.
6. Monuz, M.; Graciani, M.; Rodriguez, A.; Moya, M. L. Int J Chem Kinet 2004, 36, 634.
7. Xu, B. Q.; Aamundstad, T. A.; Lillekjendlie, B.; Bjørneboe, A.; Christophersen, A. S. Pharmacol Toxicol 1997, 80, 171.
8. Waugh, E. J.; Purchase, B. S. Biotechnol Lett 1987, 9, 151.
9. Gao, Z. H., Gu, J. Y.; Bai, X. D. Pigment Resin Technol 2007, 36, 90.
10. Gregory, P. In Encyclopedia of Chemical Technology; Kroschwitz, J. I. (Ed.); Wiley: New York, 1993; Vol. 8, p. 544.
11. Duxbury, D. F. Chem Rev 1993, 93, 381.
12. Wikipedia. Available at http://en.wikipedia.org/wiki/malachite_green. Accessed 2010.
13. Culp, S. J.; Beland, F. A. Int J Toxicol 1996, 15, 219.
14. Ritchie, C. D. J Am Chem Soc 1975, 97, 1170.
15. Ritchie, C. D.; Wright, D. J.; Huang, D. S.; Kamego, A. A. J Am Chem Soc 1975, 97, 1163.
16. Samiey, B.; Alizadeh, K.; Mousavi, M. F.; Alizadeh, N. Bull Korean Chem Soc 2005, 26, 384.
17. Caetano, W.; Tabak, M. J Colloid Interface Sci 2000, 225, 69.
18. Ritchie, C. D. Can J Chem 1986, 64, 2239.
19. Mandal, U.; Sen, S.; Das, K.; Kundu, K. K. Can J Chem 1986, 64, 300.
20. Hughes, E. D. Trans Faraday Soc 1941, 37, 603.
21. Ingold, C. K. Structure and Mechanism in Organic Chemistry; Bell: London, 1993.
22. Burton, C. A. Nucleophilic Substitution at a Saturated Carbon Atom; Elsevier: London, 1963.
23. Wyman, J. J Am Chem Soc 1933, 55, 4116.
24. Bhattacharya, A.; Das, A. K.; Kundu, K. K. Can J Chem 1981, 59, 1153.
25. Datta, J.; Kundu, K. K. Can J Chem 1981, 59, 3141.
26. Amis, E. S.; La Mer, V. K. J Am Chem Soc 1939, 61, 905.
27. Gupta, A. R. J Phys Chem 1979, 83, 2986.
28. Richardson, E. A.; Stern, K. H. J Am Chem Soc 1960, 82, 1296.
29. Wikipedia. Available at http://en.wikipedia.org/wiki/Ion-association. Accessed 2010.
30. Lide, D. L., (Ed.). CRC Handbook of Chemistry and Physics, 87th ed.; CRC Press/Taylor and Francis: Boca Raton, FL, 2006; Section 6, pp. 175–176.
31. Basu-Mullick, I. N.; Kundu, K. K. Can J Chem 1980, 58, 79.
32. Jez, J. M.; Noel J. P. J Biol Chem 2002, 277, 1369.
33. Uribe, S.; Sampedro, J. G. Biol Proced Online 2003, 5, 108.
34. Reichardt, C. Solvents and Solvent Effects in Organic Chemistry, 2nd ed.; VCH: Weinheim, Germany, 1998; pp. 189–207.
35. Meretoja, A. Acta Chem Scand 1948, 2, 352.
36. Amis, E. A.; La Mer, V. K. J Am Chem Soc 1939, 61, 905.
37. Amis, E. A.; Cook, S. E. J Am Chem Soc 1941, 63, 2621.
38. Zaghloul, A. A. Int J Chem Kinet 1997, 29, 431.
39. Ismail, A. M.; Zaghloul, A. A. Int J Chem Kinet 1998, 30, 463.
40. El-Subruiti, G. M. Int J Chem Kinet 2002, 34, 495.
41. El-Subruiti, G. M.; Chehata, A. K.; Massoud, S. S. Int J Chem Kinet 2002, 34, 1.
42. Laidler, K. J.; Landskroener, P. A. Trans Faraday Soc 1956, 52, 200.
43. Verbeek, R. M. H.; Thun, H. P.; Verbeek, F. Bull Soc Chim Belg 1977, 86, 125.
44. Åkerlof, G. J Am Chem Soc 1932, 54, 4125.
45. Hribar-Lee, B.; Dill, K. A. Acta Chim Slov 2006, 53, 257.
46. Bertrand, G. L.; Millero, F. J.; Wu, C. H.; Hepler, L. G. J Phys Chem 1966, 70, 699.
47. Davis, M. I.; Ham, E. S. Thermochim Acta 1991, 190, 251.
48. Parsons, M. T.; Lau, F. W.; Yee, E. G. M.; Koga, Y. J Solution Chem 2003, 32, 137.
49. To, E. C. H.; Davis, J. V.; Tucker, M.; Westh, P.; Trandum, C.; Suh, K. S. H.; Koga, Y. J Solution Chem 1999, 28, 1137.
50. Dohnal, V.; Roux, A.H.; Hynek, V. J Solution Chem 1994, 23, 889.
51. Matulis, D. Biophys Chem 2001, 93, 67.
52. Suppan, P.; Ghoneim, N.; Solvatochromism, N. The Royal Society of Chemistry: Cambridge, UK, 1997; p. 21.
53. Shulgin, I.; Ruckenstein, E. J Phys Chem B 1999, 103, 872.
54. Shulgin, I.; Ruckenstein, E. J Phys Chem B 1999, 103, 2496.
55. Marcus, Y. Chem Soc Rev 1993, 22, 409.
56. Marcus, Y. Monatsh Chem 2001, 132, 1387.
57. El Seoud, O. A. Pure Appl Chem 2007, 79, 1135.
58. Bosch, E.; Roses, M. J Chem Soc, Faraday Trans 1992, 88, 3541.
59. Roses, M.; Rafols, C.; Ortega, J.; Bosch, E. J Chem Soc, Perkin Trans 2 1995, 1607.
60. Tada, E. B.; Silva, P. L.; El Seoud, O. A. J Phys Org Chem 2003, 16, 691.
61. Pham, T. V.; McClelland, R. A. Can J Chem 2001, 79, 1887.